

12. X-Ray Study of the Deformation Density in Tetrafluoroterephthalodinitrile: Weak Bonding Density in the C, F-Bond¹⁾

by Jack D. Dunitz, W. Bernd Schweizer and Paul Seiler

Laboratorium für Organische Chemie, ETH-Zentrum, CH-8092 Zürich

(6.X.82)

Summary

A careful deformation density study of tetrafluoroterephthalodinitrile at 98K has been made from X-ray diffraction measurements. Prominent 'bonding density' peaks are found at or near the mid-points of the C, C- and C, N-bonds but not for the C, F-bonds, which show only weak density. Similarly weak bonding densities for C, F-bonds are also found for 1,1,4,4-tetrafluorocyclohexane. The possible significance of these results in terms of bonding theory is briefly discussed.

The electron-density distribution is the most detailed information obtainable from X-ray diffraction experiments. In favorable circumstances, it can be measured with sufficient accuracy to detect features of chemical interest, such as bonding and lone-pair densities, even in moderately complicated organic molecules. Since these chemically interesting features are small compared with the total charge density they are most conveniently depicted in terms of a difference density: the difference between the observed density ρ_o and the superposition of the spherically averaged free-atom densities ρ_c . This difference density, sometimes known as the deformation density or bonding density, describes the change in electron density associated with formation of the molecule from the free atoms. It is conveniently calculated by Fourier summation with coefficients $F_H(obs) - F_H(calc)$ where $F_H(obs)$ are structure amplitudes observed in an X-ray diffraction experiment and the calculated quantities $F_H(calc)$ depend on a knowledge of the free-atom X-ray scattering factors [2] and on the positional and vibrational parameters assigned to the individual atoms, quantities that must also be determined by experiment. This may be a neutron-diffraction experiment, in which case the difference function is often referred to as an X-N density, or it may be the same X-ray experiment as used to provide the structure amplitudes, thus yielding an X-X density. The X-ray experiment can only perform this double duty effectively if high-order diffraction data can be measured. This is because the effect of valence deformation on the free-atom scattering factors decreases with increasing scattering angle and becomes

¹⁾ A preliminary account of this work was presented at the 12th International Congress of Crystallography, Ottawa, Canada, 16-25 August 1981 [1].

negligible at sufficiently high scattering angle, where, essentially, only the inner-core electrons still scatter in phase. Thus, unbiased estimates of the atomic positional and vibrational parameters are obtainable in principle from least-squares refinement of high-order data. The deformation density itself, however, depends heavily on the low-order data. For molecular crystals, in order to obtain sufficiently extensive high-order X-ray data, it is usually necessary to reduce the atomic vibration amplitudes by cooling the crystals during the X-ray measurements.

In the main part of this paper we present results from an accurate, low-temperature study of tetrafluoroterephthalodinitrile (hereafter TFT) using high-order X-ray data. The crystal structure at room temperature was recently determined by *van Rij & Britton* [3] who pointed out the suitability of this material for a low-temperature charge-density study. The molecule contains no H-atoms; all the atoms are of approximately equal scattering power for X-rays; the molecular crystallographic site symmetry is $C_{2h}(2/m)$ which reduces the number of independent parameters to be determined. Since we were interested in making a charge-density study of a molecule containing highly polar bonds, we decided to take up the problem where *van Rij & Britton* had left it.

Crystallographic data for tetrafluoroterephthalodinitrile (TFT), $C_8F_4N_2$. Orthorhombic, cell dimensions at 98 K: $a = 7.6848(4)$, $b = 9.7350(6)$, $c = 9.5549(7)$ Å (for room-temperature values see [3]); space group $Cmca$, $Z = 4$, $D_c = 1.790$ Mg m⁻³.

Experimental part. – Our sample of TFT was obtained from Professor *Doyle Britton*. All X-ray measurements were carried out on an *Enraf-Nonius CAD4* automatic diffractometer equipped with graphite monochromator (MoK α radiation, $\lambda = 0.71069$ Å) and cooling device. Two independent data sets were collected, both at 98K. Since our final results are based mainly on the second set, extending to $s = \sin\theta/\lambda = 1.15$ Å⁻¹, we restrict ourselves here to the experimental details for this.

The material was recrystallized by slow evaporation of an acetone solution at *ca.* -20°. Considerable attention was paid to the choice of a crystal for intensity measurements. About 20 crystal specimens were mounted on the diffractometer, cooled to 98K, and tested for their general diffraction behaviour. The crystal finally selected (dimensions *ca.* 0.45 × 0.35 × 0.3 mm) had a mosaic spread smaller than the divergence of the primary beam (<0.2 peak half-width at half-height) and showed minimal intensity fluctuations when rotated round the diffraction vector **H** for several reflections.

Three standard reflections: 10,0,0 ($s = 0.651$ Å⁻¹), 333 and 333 ($s = 0.294$ Å⁻¹) were monitored 221 times at intervals of 15×10^3 s radiation time; they showed a slow intensity decrease amounting to about 8% at the end of the measurement period (about 6 weeks elapsed time). A correction was made to compensate for this slow intensity drift.

A total of 17740 intensity measurements (ω, θ -scans) were made, extending to $s = 1.15$ Å⁻¹. These were reduced to 2387 symmetry-independent reflections, of which 1580 had $I > 3\sigma(I)$ with $\sigma(I)$ estimated as $(P + B + 2.2 \times 10^{-4} I^2)^{1/2}$ where P = integrated peak intensity, B = sum of background counts at each end of scan, $I = P - B$. Since, in general, all eight symmetry-equivalent aspects of each hkl reflection were measured, this estimate of $\sigma(I)$ could be checked by comparison with the actual standard deviations of individual intensity measurements from corresponding mean values. The overall agreement was satisfactory. From the many multiple measurements we obtained an R -value for the internal consistency of the intensity measurements (*Eqn. 1*):

$$R = \frac{\sum_H \sum_n |I_H^n - \langle I_H \rangle|}{\sum_H \langle I_H \rangle} = 0.016 \quad (1)$$

where n is the multiplicity of the reflection H . The averaged intensities were reduced to F -values in the usual way, but absorption corrections were considered to be unnecessary ($\mu = 1.92$ cm⁻¹).

The room-temperature structure described by *van Rij & Britton* [3] served as starting-point for a long series of least-squares refinements employing different ways of selecting and weighting the diffraction data (full details of these comparisons will be published elsewhere). Our final positional and vibrational parameters, listed in *Table 1*, are based on full-matrix least-squares analysis of 527 high-order reflections with $F > 20\sigma(F)$ in the range $0.85 \text{ \AA}^{-1} < s < 1.15 \text{ \AA}^{-1}$ using atomic scattering factors of *Cromer & Mann* [4] and standard weights, $w = 1/(\sigma^2(F))$, leading to $R = 0.013$ for the reflections involved ($R = 0.022$ including isotropic extinction correction for all 1269 reflections with $F > 20\sigma(F)$). The corresponding difference map in the molecular plane, calculated with the same subset of 572 reflections, is shown in *Figure 1*. Its essentially flat, featureless nature confirms that this high-order data subset is well represented by the free-atom scattering factors [4] and contains essentially no information about the deformation density.

Parallel calculations based on the same range of s but with less stringent data selection (*i.e.* including a larger number of reflections) led to positional parameters identical within 0.002 Å with those of *Table 1* but with slightly smaller standard deviations. The vibrational parameters tend

Table 1. Atomic coordinates and vibration parameters (all $\times 10^5$) with standard deviations in parentheses

	x	y	z	U_{11}	U_{22}	U_{33}	U_{12}	U_{13}	U_{23}
C(1)	15651(4)	5912(2)	4021(2)	982(6)	955(7)	1068(6)	-92(6)	-39(6)	-79(4)
C(2)	0	11978(4)	8083(4)	1133(10)	816(9)	924(10)	0	0	-81(7)
C(3)	0	24201(4)	16332(4)	1756(11)	938(9)	1061(10)	0	0	-188(7)
F(1)	30608(3)	11524(3)	7931(3)	1076(6)	1663(8)	1800(9)	-364(5)	-203(5)	-283(6)
N(1)	0	34107(4)	22962(5)	2956(22)	1237(10)	1557(12)	0	0	-560(9)

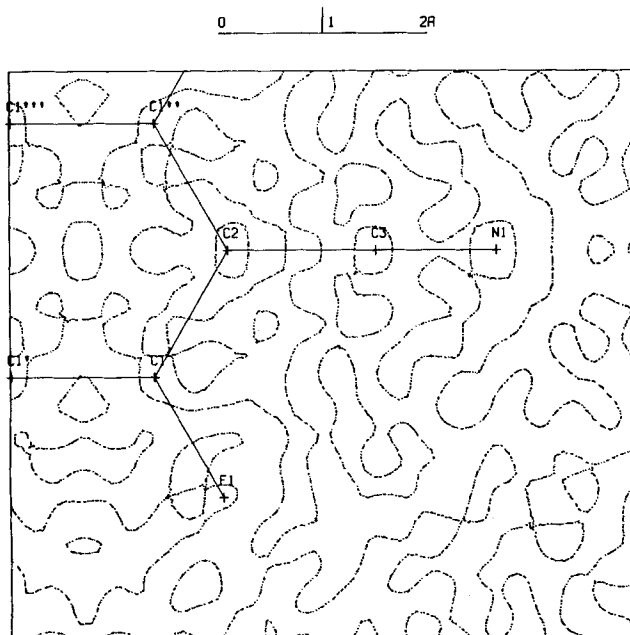


Fig. 1. Tetrafluoroterephthalodinitrile (TFT): charge-density difference map in the molecular plane calculated with the subset of 527 reflections with $F > 20\sigma(F)$ in the range $0.85 \text{ \AA}^{-1} < \sin\theta/\lambda < 1.15 \text{ \AA}^{-1}$. Contours are drawn at intervals of $0.075 e \text{ \AA}^{-3}$ but the map is so flat that only the zero contour appears, *i.e.* the high-order reflections do not contribute much to the charge-deformation density (compare Fig. 2).

to show a slight systematic increase as more reflections of diminished accuracy are added; for the calculation with all 1406 measured reflections in the $0.85\text{--}1.15\text{ \AA}^{-1}$ range, the diagonal elements of the vibrational tensors are uniformly about one standard deviation larger than those reported in *Table 1*. The corresponding difference map (not shown here) contains a good deal of noise but there is no improvement in information compared with *Figure 1*. To check that the atomic positional and vibrational parameters did not depend on the choice of atomic scattering factors, another parallel set of calculations was made with the scattering factors of *Doyle & Turner* [5] based on relativistic *Hartree-Fock* wave functions. The results (also the difference maps) were indistinguishable from those obtained with the *Cromer-Mann* scattering factors [4].

Molecular geometry and packing. – Bond lengths and angles derived from our analysis are shown in *Figure 2* together with values corrected for librational motions²⁾. The molecular dimensions are very similar to those obtained earlier by *van Rij & Britton* [3] and indeed become virtually identical with those when libration corrections are applied to both sets. The molecule has crystallographic $C_{2h}(2/m)$ site symmetry, but it has virtual $D_{2h}(mmm)$ symmetry, the largest deviations from the mean plane being 0.011 \AA for the F- and 0.008 \AA for the N-atoms.

As there is no phase transition between room temperature and 98K the packing at the lower temperature is essentially the same as described by *van Rij & Britton* [3]. The angle between the normal to the molecular plane and the *c* axis is 34.4° at room temperature and 33.6° at 98 K. Nevertheless, since the cell volume contracts by 3.7% while the molecular dimensions remain constant, the distances between neigh-

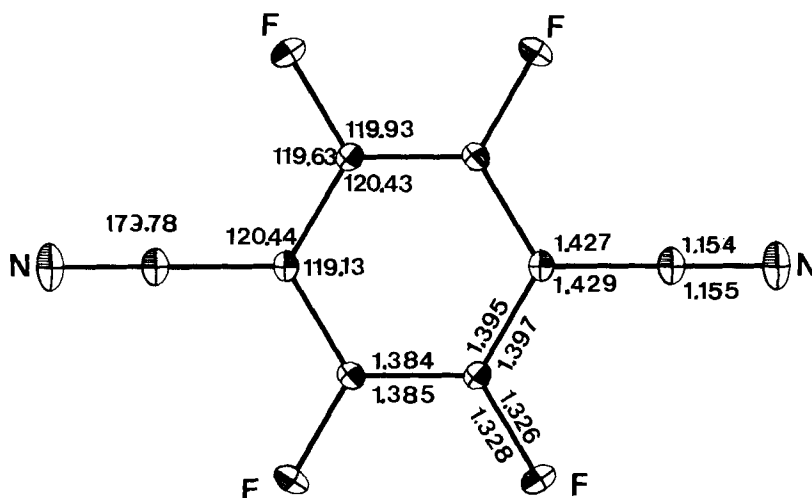


Fig. 2. *Molecular geometry and vibration ellipsoids* (50% probability level) at 98 K. Bond lengths (in Å) have standard deviations of less than 0.001 \AA ; the upper figures refer to uncorrected values, the lower ones are corrected for librational motion. Bond angles (in deg) have standard deviations of $0.02\text{--}0.04^\circ$.

²⁾ The estimated standard deviations in bond lengths lie in the range $0.0003\text{--}0.0006\text{ \AA}$. On purely statistical grounds it might appear justifiable to add another significant figure to the values cited in *Fig. 2*. However, since the bond lengths also depend on the cell constants and the atomic positions are complicated averages over many vibrational states and the libration corrections are only approximate, the meaning of the extra significant figure would be somewhat questionable.

bonding molecules must become smaller on the whole, and it is of interest to examine which types of these intermolecular distances are most affected. From *Table 2* it is seen that the shortest intermolecular distance at room temperature ($F \cdots F$, 3.10 Å) suffers the greatest contraction, while the relatively longer $F \cdots C$ and $N \cdots C$ distances change much less on cooling. These facts can be rationalized to some extent in terms of standard non-bonded atomic radii [6]. However, a detailed, quantitative explanation of the temperature dependence of the crystal packing would require a much more thorough analysis, which we have no intention of making at present.

Thermal motion analysis. – Preliminary analysis of the atomic vibration tensors (*Tab. 1*) shows that *Hirshfeld's* rigid-bond test [7] and its generalization to cover overall molecular rigidity [8] are both satisfied rather well. The largest differences between mean-square vibrational amplitudes of pairs of atoms along their respective interatomic vectors are 7×10^{-4} Å² for the bonded pair C(1), F(1) and $8-9 \times 10^{-4}$ Å² for non-bonded pairs. The three largest differences all involve the N-atom, and it is evident from the tensor components listed in *Table 1* that this atom has an abnormally large U_{11} -component, corresponding to vibration normal to the C(3), N-direction and in the molecular plane. This suggests that one of the two bending vibrations of the nitrile group, the in-plane vibration, may be contributing significantly to the observed U_{ij} -values.

Table 3 shows that introduction of this internal molecular motion using the simple one-parameter model of *Dunitz & White* [9] leads to a considerable improvement in the agreement between observed and calculated tensor components compared with the rigid-body vibration model alone: a reduction in the r.m.s. discrepancy from 5.6×10^{-4} Å² to 4.4×10^{-4} Å² for an increase in the number of adjustable parameters from 8 to 9. The value obtained for the mean-square bending amplitude is $5.0(2.1)$ deg², corresponding to a nominal force constant³⁾ of about $160 \text{ J mol}^{-1} \text{ deg}^{-2}$ ($\approx 0.9 \text{ m dyn} \cdot \text{Å rad}^{-2}$). This is at best only a very rough estimate, which appears somewhat high compared with the value of $0.35 \text{ m dyn} \cdot \text{Å rad}^{-2}$ for the in-plane bending force constant of the cyano group in benzonitrile [10]. The two values refer to different molecules in different aggregation states and are only rough estimates, but at least they are of the same order of magnitude.

As far as the molecular rigid-body motion is concerned, the translational vibrations are seen from *Table 3* to be fairly isotropic, in contrast to the librations. The largest librational amplitude is round the long molecular axis, while the smallest is round the other inertial axis in the molecular plane, corresponding to the [100] crystal direction.

³⁾ The possibility of deriving force constants for internal molecular vibrations from atomic vibration tensors obtained by X-ray or neutron diffraction studies does not seem to be well known. A recent study [11] of data from 125 crystal structure analyses concludes that this method should be a valuable complement to other methods of studying torsional and other relatively soft intramolecular motions, besides its use as a probe of intermolecular potential functions. The present application to the in-plane bending vibration of the cyano group may not be too meaningful since other intramolecular vibrations of comparable frequency can also be expected to contribute significantly to the observed U_{ij} -values.

Table 2. Short intermolecular distances (in Å) at room temperature and at 98 K

Type	RT.	98 K	Direction cosines ^{a)}			Radius sum (Å) ^{b)}
F...F	3.096	2.980	1,	0,	0,	2.94
	3.180	3.150	0.274,	-0.833,	0.481	
N...F	3.251	3.223	0.462,	0.682,	-0.567	3.02
C(3)...F	3.175	3.087	0.483,	-0.450,	0.751	3.17
	3.191	3.129	0.380,	0.394,	-0.786	
C(2)...N	3.316	3.262	0,	0.832,	-0.555	3.25
C(1)...N	3.347	3.285	0.366,	0.646,	-0.669	

^{a)} Relative to the *a, b, c* crystal axes, respectively. The values given are for the 98 K analysis.

^{b)} Using atomic radii of 1.47 Å for F, 1.55 Å for N and 1.70 Å for C, as in the compilation by Bondi [6].

Table 3. Analysis of the atomic vibration tensors. Model 1 treats the molecule as a rigid body, model 2 includes the in-plane bending vibration of the nitrile group with the motion imparted only to the N-atom.

Crystal coordinate system	Model 1	Model 2
L_{11} (deg ²)	2.32(10)	2.32(10)
L_{22}	5.59(19)	5.55(19)
L_{23}	1.33(12)	1.39(12)
L_{33}	5.05(14)	4.97(14)
T_{11} ($\times 10^{-5}$ Å ²)	885(14)	888(14)
T_{22}	771(15)	775(15)
T_{23}	1(13)	4(13)
T_{33}	776(19)	778(19)
$\langle \vartheta^2 \rangle$ (deg ²)	-	5.0(2.1)
Molecular inertial coordinate system ^{a)}		
L_{11} (deg ²)	6.65	6.66
L_{13}	-0.27	-0.28
L_{22}	2.32	2.32
L_{33}	4.00	3.86
$\langle (\Delta U_{ij})^2 \rangle^{1/2}$	5.6×10^{-4} Å ²	4.4×10^{-4} Å ²

^{a)} The molecular axes are numbered in order of increasing moment of inertia: axis 1 is the long direction of the molecule, axis 2 bisects the C(1), C(1')-bond, and axis 3 is perpendicular to the molecular plane.

Difference densities. – Figure 3 shows an X–X difference map in the molecular plane and based on the 1269 reflections with $F(\text{obs}) > 20 \sigma(F)$. Difference maps calculated with less stringent inclusion criteria do not differ from Figure 3 in any important respects but contain more noise in the form of minor peaks and troughs. Similarly, maps based on the slightly different values of the positional and vibrational parameters that were obtained from other high-order refinements or on different choices of atomic scattering factors are also similar to Figure 3 in all essential features. We can therefore afford to have considerable confidence in the main qualitative traits of the charge-difference distribution portrayed in Figure 3. Clearly, there are prominent peaks for the ‘bonding’ densities of the three crystallo-

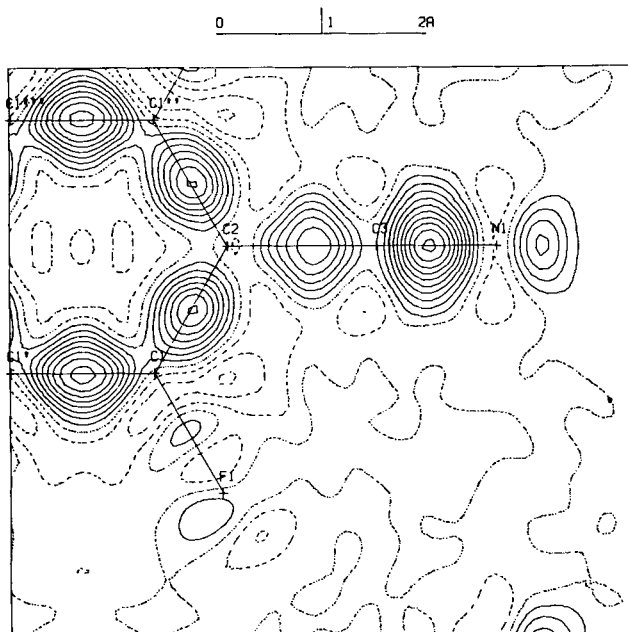


Fig. 3. Tetrafluoroterephthalodinitrile: charge-density difference map in the molecular plane calculated with 1269 reflections with $F > 20\sigma(F)$. Contours are drawn at intervals of $0.075e \cdot \text{\AA}^{-3}$, positive contours full lines, negative contours dashed, zero contour dotted. Note the weak density in the C,F-bond.

graphically different kinds of C,C-bond, for the C,N-triple bond, for the lone-pair density at the N-atom, but, conspicuously, not for the C,F-bond.

Sections of the X–X map perpendicular to the molecular plane and passing through the mid-points of the C,C- and C,N-bonds are shown in Figure 4. The bonds in the benzene ring show the expected extension of the density peaks in the direction normal to the molecular plane, while the contours of the exocyclic C,C-bond and of the C,N-triple bond are essentially circular, the density in the triple bond being appropriately higher than in the single bond. A similar distinction between elliptical and circular contours in the deformation densities of different kinds of bond has been noted in an earlier X–X study of tetraphenylbutatriene [12] but using the approach where the deformation density is expressed in parametric form and refined by least-squares analysis, together with the usual positional and vibrational parameters [13]. The fact that our unparametrized peaks are virtually as smooth as those obtained by least-squares modelling in the other approach speaks for the low noise-level of our difference maps.

A similar deficit of deformation density in C,F-bonds has also been observed in a difference map calculated for 1,1,4,4-tetrafluorocyclohexane [14] in this laboratory⁴).

⁴) The molecular parameters on which this difference map is based were derived from X-ray data extending to $s = 0.90 \text{ \AA}^{-1}$ [14]. The data are less accurate than in the present study but good enough to show the difference between C,C- and C,F-bonding densities.

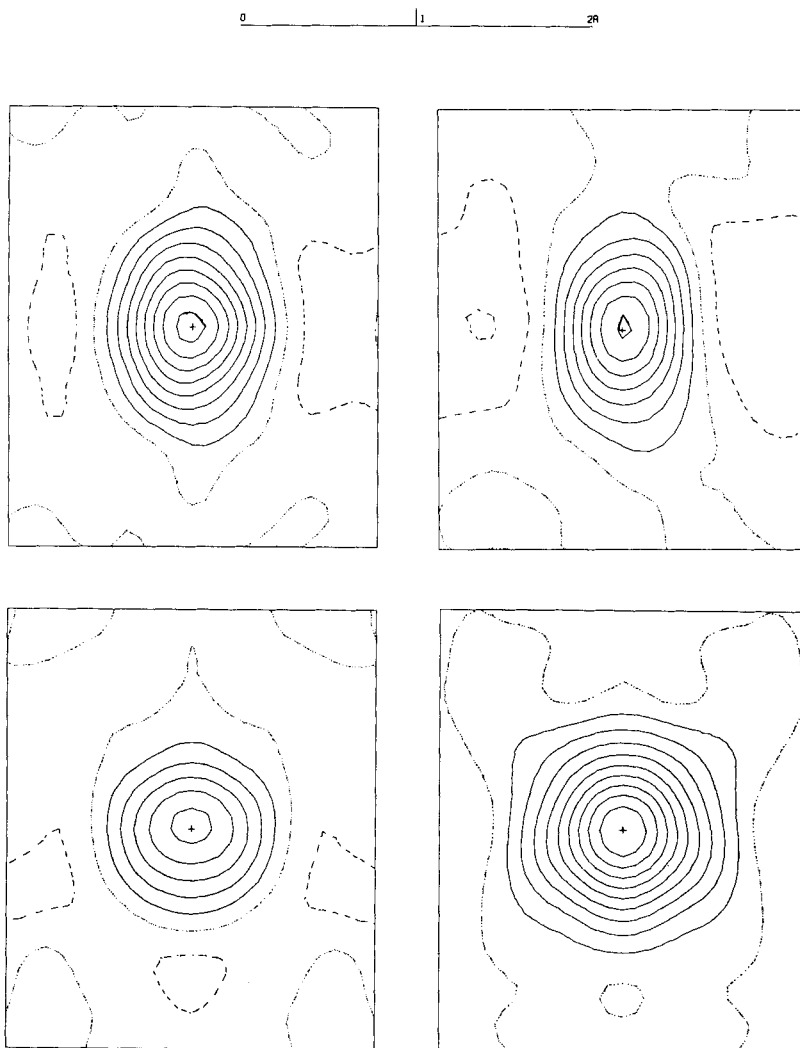


Fig. 4. Tetrafluoroterephthalodinitrile: sections of charge-density difference map perpendicular to the molecular plane and passing through the midpoints of the bonds (top left: C(1),C(1'); top right: C(1),C(2); bottom left: C(2),C(3); bottom right, C(3),N). In each section the direction of the molecular plane is horizontal. Details of calculation as in Figure 2.

Figure 5 shows the difference density in the C,C,C- and F,C,F-planes in this molecule; it is immediately obvious that the density in the C,F-bonds is virtually non-existent compared with that in the C,C-bonds.

What is so special about the C,F-bonds in these molecules? Why, in contrast to the other bonds, do they not show any appreciable 'bonding' density? Two properties of the C,F-bond suggest themselves immediately as being possibly relevant in this context. One is the highly polar nature of the C,F-bond, the other

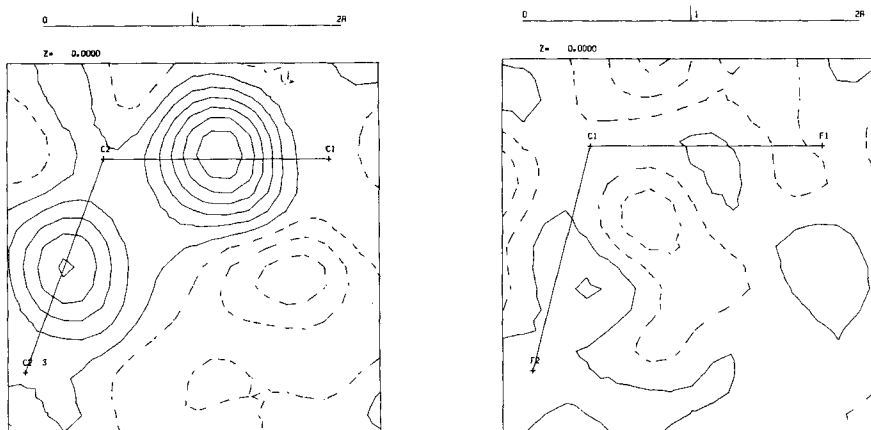


Fig. 5. 1,1,4,4-Tetrafluorocyclohexane: charge-density difference map in the C, C, C- and F, C, F-planes calculated with 723 reflections with $F > 20\sigma(F)$. Contours are drawn at intervals of $0.075e \text{ \AA}^{-3}$, positive and zero contours full lines, negative contours dashed.

is the electron-richness of the F-atom compared with the other atoms; the difference map clearly depends not only on how much charge density is present in the binding region but also on how much is subtracted out.

The second factor seems to be much more important, judging from the results of several recent deformation-density studies. For example, while the 'bonding' density of the C, O-single bonds in 1,4,7,10,13,16-hexaoxacyclooctadecane (18-crown-6) is low compared with that of the C, C-bonds [15], the same is true for the iso-electronic N, N'-single bonds in N, N'-diformylhydrazine [16], tetraformylhydrazine [17]⁵⁾, and carbonohydrazide [18]. An even weaker peak is observed in both X-X and X-N maps for the O, O-bond density in hydrogen peroxide [19]. Very recently (Seiler & Dunitz, unpublished results) we have shown that the deformation density of the several types of bond present in 1,2,7,8-tetraaza-4,5,10,11-tetraoxatricyclo[6.4.1.1^{2,7}]tetradecane [20] decreases in the order C, N > C, O > N, N > O, O with even a slightly negative density at the centre of the O, O-bond. The deformation density found for the C, F-bond in the present study fits very nicely into this sequence.

The occurrence of only an extremely weak or even slightly negative 'bonding' density at the middle of a chemical bond may appear to run counter to the current conventional wisdom about the nature of the chemical bond. Residual density peaks between pairs of conventionally bonded atoms are often regarded as a kind of experimental corroboration of the view that chemical binding results from transfer of charge from non-bonding regions of space to the internuclear region. This view seems to be based on the tacit assumption that all electron-pair bonds are essentially of the same nature as the bond in the H₂-molecule. However, since the analysis by Bader *et al.* of Hartree-Fock charge distributions in first-row diatomics

⁵⁾ These two compounds are indicated in the literature as s-diformo- and tetraformohydrazide, respectively.

and hydrides [21], it can be asserted that the H_2 -molecule does not provide a good basis for the discussion of chemical binding in general. For the homonuclear diatomic molecules, only Li_2 fitted the simple picture of removal of charge from the antibinding region and a buildup in the binding region; for the other members, the binding region was increasingly depleted of charge density. These analyses were based on valence-state densities for the isolated atoms; if spherical atoms were used as the basis for comparison, as in the experimental difference maps discussed here, the depletion of charge in the overlap region between electron-rich atoms would be still more extreme.

A careful analysis of the binding energy in first-row hydrides and homonuclear diatomic molecules indicates that the H_2 -molecule, far from being the paradigm, is in many respects atypical and unsatisfactory for a general discussion of the chemical bond. According to *Hirshfeld & Rzotkiewicz* [22], the classical interaction of two spherically averaged ground-state atoms is *always* binding. Indeed, for the homonuclear diatomics, except H_2 , the classical promolecule is considerably more stable than the *Hartree-Fock* molecule. However, the superposition of spherical free-atom densities in the overlap region between electron-rich atoms such as F is opposed by the exclusion principle. Thus a molecule like F_2 can be said to be stable because it just manages to survive the unfavourable charge redistribution required by the exclusion principle.

The absence of any appreciable lone-pair density at the F-atom can be understood in terms of the large electronegativity of this atom. Calculated density difference maps of near *Hartree-Fock* quality [21] show that in the homonuclear diatomic molecules from N_2 to F_2 the lone-pair densities contract more and more towards the nuclei. They therefore become more and more difficult to resolve from the spherical free-atom density that is subtracted out in the difference map. A neutron-diffraction study might help to resolve this problem.

The fact that electron-density difference maps depend just as much on what is subtracted out as on the total charge density raises questions about what is to be learned from such maps. Is the absence of 'bonding' density in C, F- and other bonds involving electron-rich atoms to be regarded as an apparently paradoxical although trivial consequence of the method or as an indication of a deep-seated flaw in the conventional model of the chemical bond? The choice of spherical atoms as the basis for comparison can be questioned but it is the only choice that allows fully for the reduction of symmetry that occurs when the free atom becomes part of a bound system. Besides, this choice is by far the most convenient because of the easy availability of spherically symmetric scattering factors. The use of non-spherical valence-state densities must involve certain preconceptions about the nature of the charge redistribution on molecule formation. In the present analysis, for example, we could doubtless produce difference maps showing residual density in the C, F-bonding region by subtracting out not spherical atoms but specially prepared ones with a deficiency of density in the bonding direction. It is difficult to see what would be gained by such a manoeuvre. At present, it seems much more preferable to stick to spherical atoms as the basis for comparison, at least until we have enough experience with many different kinds of bond to understand better the possibilities and limitations of the method.

REFERENCES

- [1] *J. D. Dunitz, W. B. Schweizer & P. Seiler, Acta Crystallogr. A37, C-129 (1981).*
- [2] *International Tables for X-ray Crystallography, Volume 4, Chapter 2.2. Kynoch Press: Birmingham, 1974.*
- [3] *C. van Rij & D. Britton, Cryst. Struct. Comm. 10, 175 (1981).*
- [4] *D. T. Cromer & J. B. Mann, Acta Crystallogr. A24, 321 (1968).*
- [5] *P. A. Doyle & P. S. Turner, Acta Crystallogr. A24, 390 (1968).*
- [6] *A. Bondi, J. Phys. Chem. 68, 441 (1964).*
- [7] *F. L. Hirshfeld, Acta Crystallogr. A32, 239 (1976).*
- [8] *R. E. Rosenfield, K. N. Trueblood & J. D. Dunitz, Acta Crystallogr. A34, 828 (1978).*
- [9] *J. D. Dunitz & D. N. J. White, Acta Crystallogr. A29, 93 (1973).*
- [10] *A. Kuwal & K. Michada, Spectrochim. Acta A35, 841 (1979).*
- [11] *K. N. Trueblood & J. D. Dunitz, Acta Crystallogr., in press.*
- [12] *Z. Berkovitch-Yellin & L. Leiserowitz, J. Am. Chem. Soc. 97, 5627 (1975).*
- [13] *F. L. Hirshfeld, Acta Crystallogr. B27, 769 (1971).*
- [14] *J. D. Dunitz, W. B. Schweizer & P. Seiler, Helv. Chim. Acta 66, 134 (1983).*
- [15] *E. Maverick, P. Seiler, W. B. Schweizer & J. D. Dunitz, Acta Crystallogr. B36, 615 (1980).*
- [16] *H. Hope & T. Otterson, Acta Crystallogr. B35, 370 (1979).*
- [17] *T. Otterson, J. Almlöf & J. Carle, Acta Chem. Scand. A36, 63 (1982).*
- [18] *T. Otterson & H. Hope, Acta Crystallogr. B35, 373 (1979).*
- [19] *J. M. Savariault & M. S. Lehmann, J. Am. Chem. Soc. 102, 1298 (1980).*
- [20] *S. N. Whittleton, P. Seiler & J. D. Dunitz, Helv. Chim. Acta 64, 2614 (1981).*
- [21] *R. F. W. Bader, W. H. Henneker & P. E. Cade, J. Chem. Phys. 46, 3341 (1967); R. F. W. Bader, I. Keaveny & P. E. Cade, ibid. 47, 3381 (1967); R. F. W. Bader & A. D. Bandrauk, ibid. 49, 1653 (1968).*
- [22] *F. L. Hirshfeld & S. Rzotkiewicz, Mol. Phys. 27, 1319 (1974).*